Electronic Supplementary Material (ESI) for New Journal of Chemistry.


# Skillfully Manipulating Electron Transitions of Au Nanoparticles for Modulation of Nanozyme Functions

Ying Li*, Yujie Chen, Kaiyuan Wang, Yufeng Zhou, Wei Wei, Yuanjian Zhang and Songqin Liu

Jiangsu Engineering Laboratory of Smart Carbon-Rich Materials and Device, School of Chemistry and Chemical Engineering, Southeast University, Nanjing 211189, China.

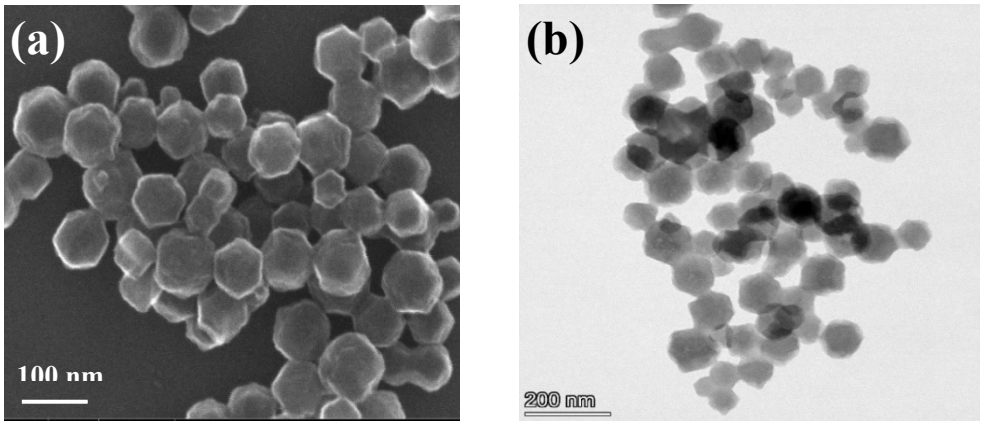


Figure S1 (a) SEM image and (b) TEM image of CZIF-800.

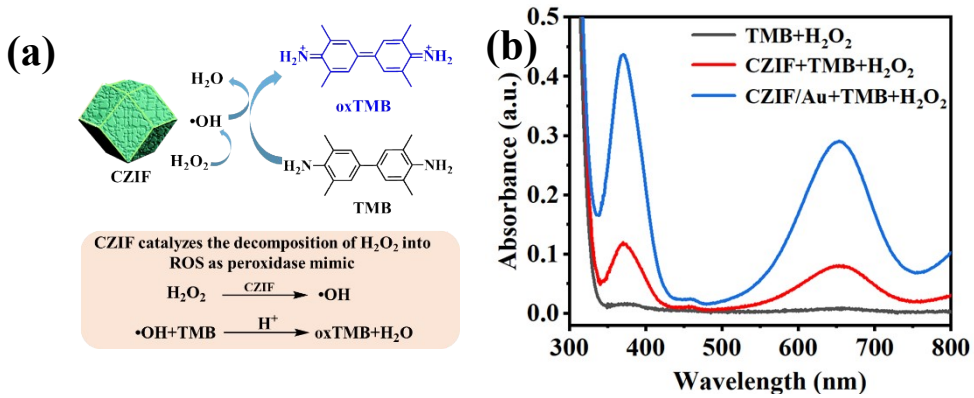


Figure S2 (a) Schematic illustration of the catalytic mechanism of peroxidase-mimic CZIF nanozyme. (b) UV-*vis* spectra of TMB oxidation in solutions with different components after incubation at 37 ℃ for 15 min.

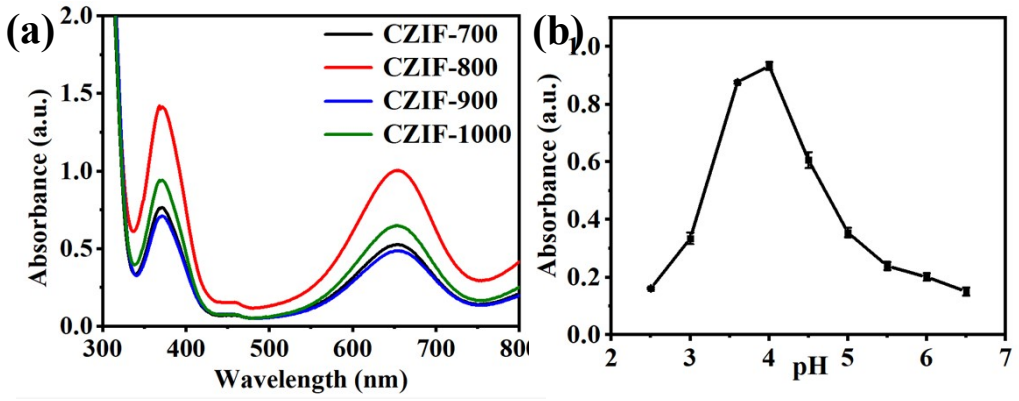


Figure S3 (a) Effect of pyrolysis temperatures and (b) pH of catalytic reaction solutions on the peroxidase-like activity of CZIF.

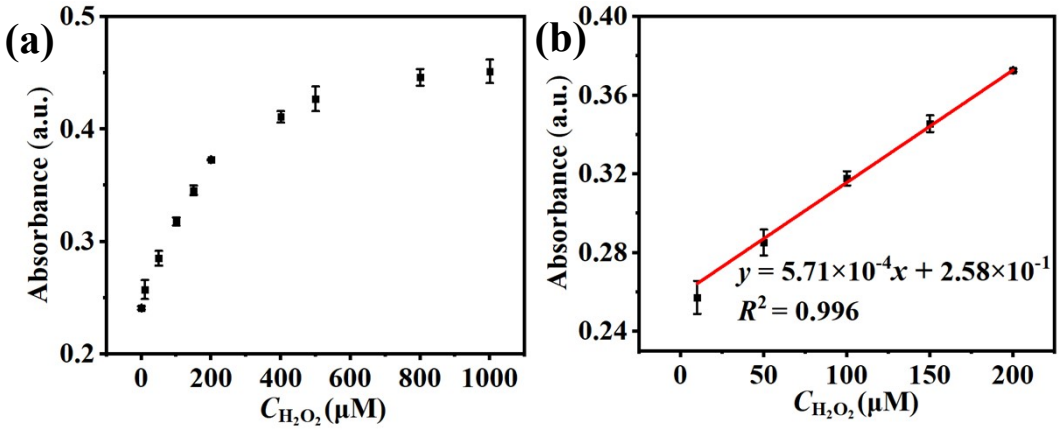


Figure S4 (a) Dose-response curves for $H_2O_2$ using CZIF as a peroxidase-mimic nanozyme. (b) Linear calibration plots of $H_2O_2$, error bars representing the standard deviation of three parallel samples.

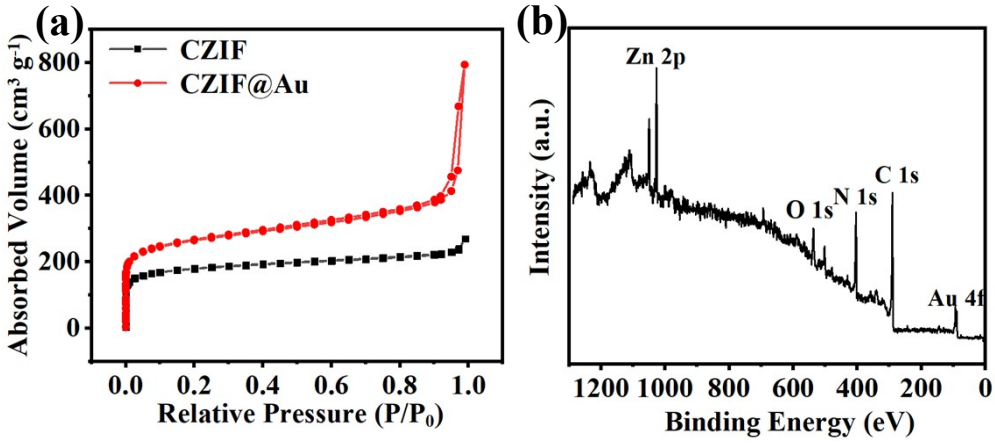


Figure S5 (a) $N_2$ adsorption-desorption isotherms of CZIF/Au and CZIF. (b) XPS survey spectrum of CZIF/Au.

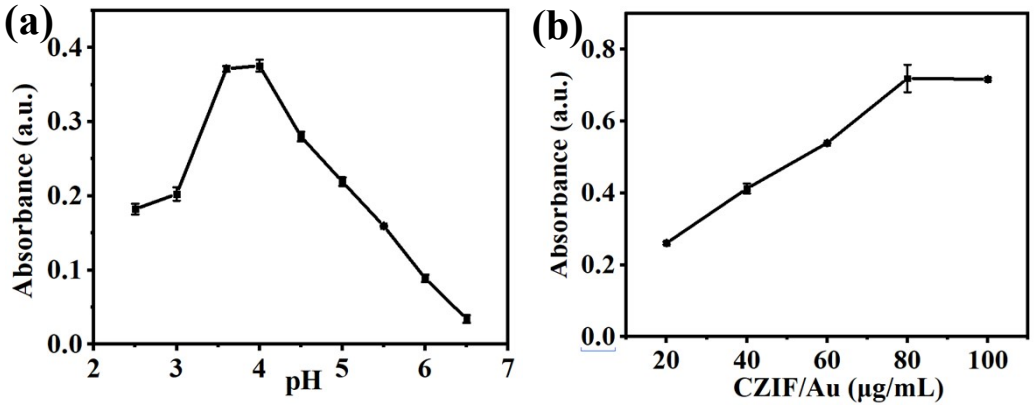


Figure S6 Effect of (a) pH of reaction solutions and (b) concentrations of substrates on the peroxidase-like activity of CZIF/Au.

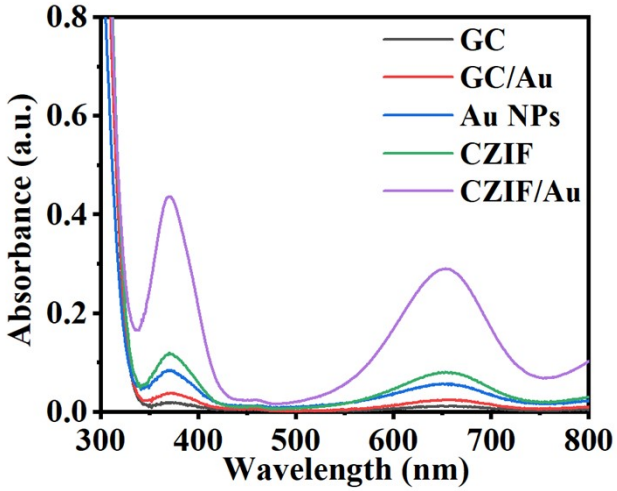


Figure S7 UV-*vis* spectra of TMB oxidation catalyzed by graphite carbon (GC), GC/Au, Au NPs, CZIF and CZIF/Au after incubation at 37 ℃ for 15 min.

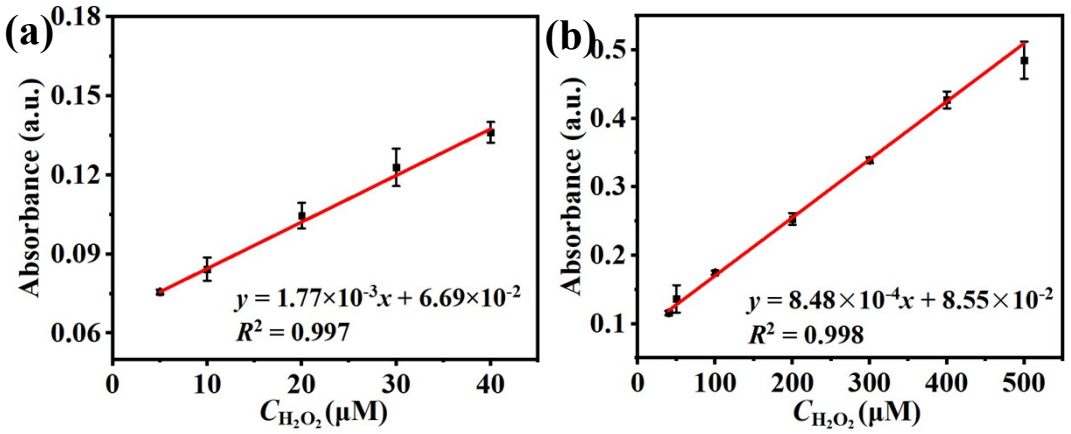


Figure S8 Linear calibration plots of detection of $H_2O_2$ in the dark using CZIF/Au in (a) low concentration range and (b) high concentration range, error bars representing the standard deviation of three parallel samples.

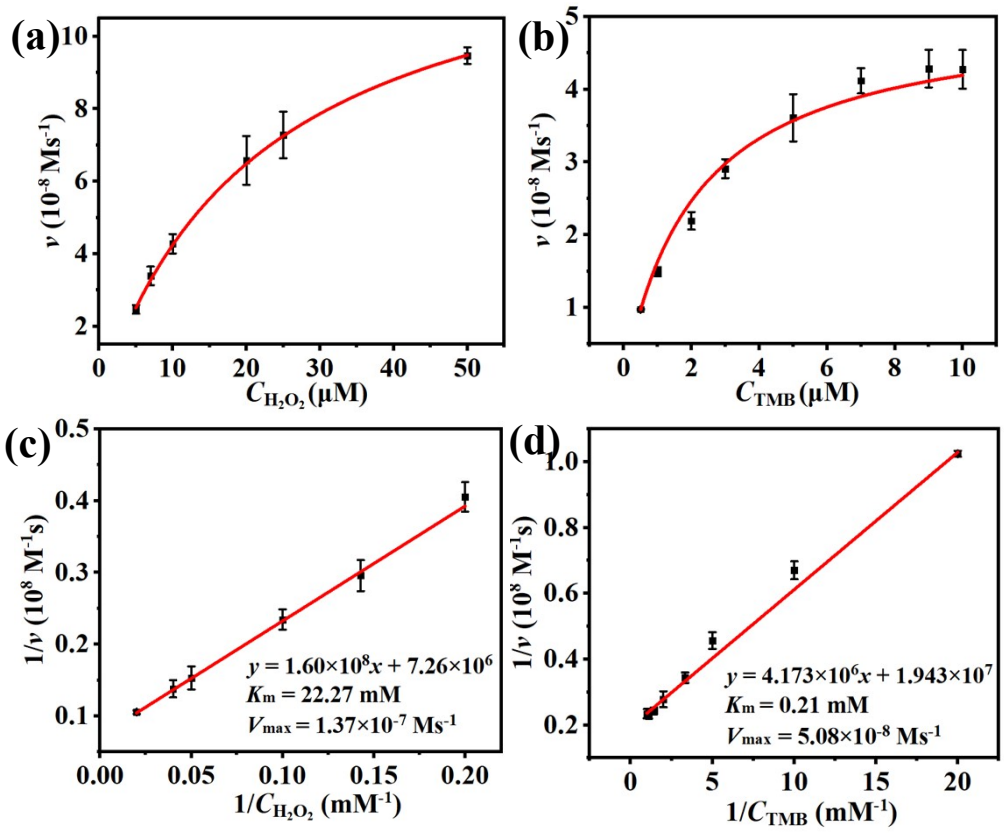


Figure S9 Steady-state dynamic determination of CZIF/Au, (a) fixing TMB concentration as 1 mM and (b) fixing $H_2O_2$ concentration as 10 mM. Double-reciprocal equation plots of the CZIF/Au activity (c) for $H_2O_2$ and (d) for TMB.

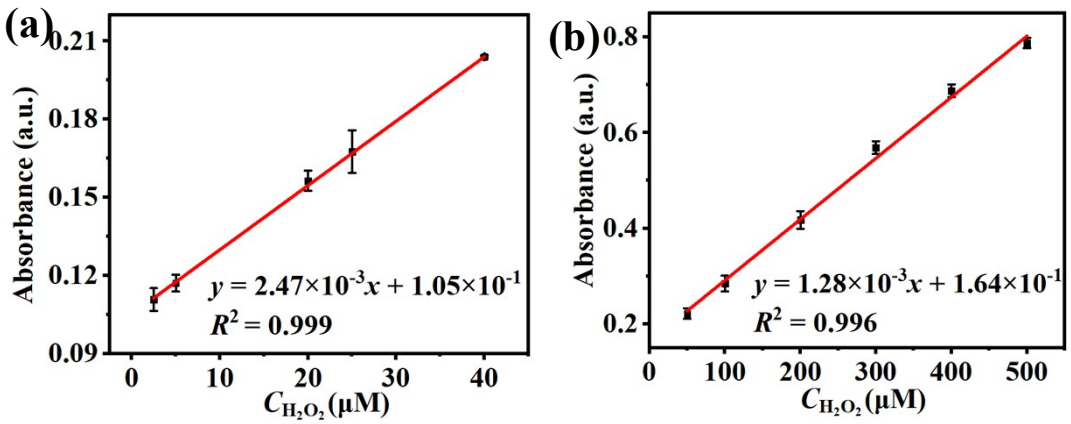


Figure S10 (a) Linear calibration plots of detection of $H_2O_2$ upon 655 nm irradiation in (a) low concentration range and (b) high concentration range, error bars representing the standard deviation of three parallel samples.

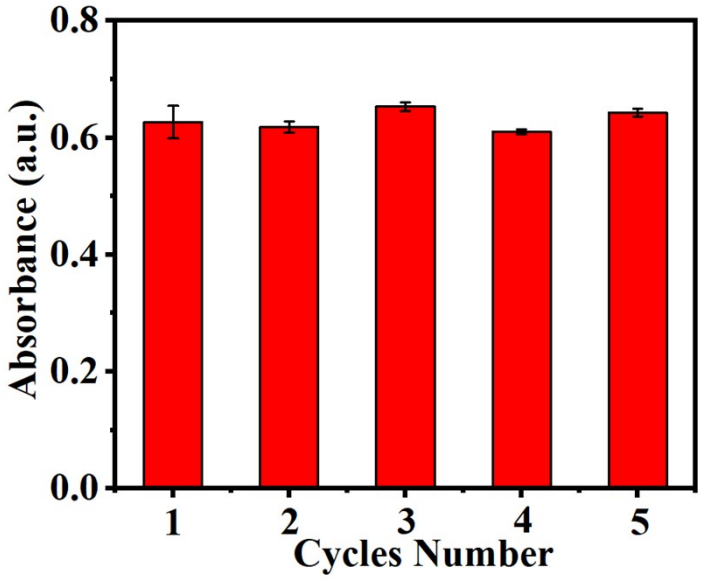


Figure S11 The stability of the CZIF/Au after five times cycles.

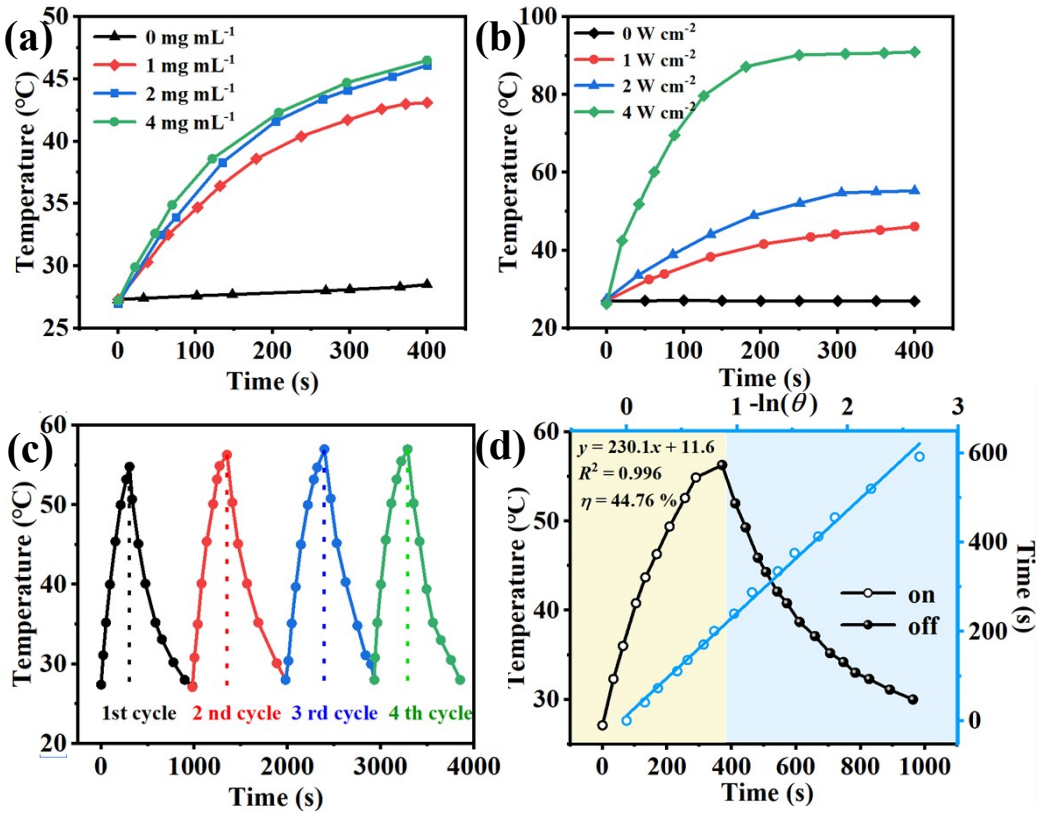


Figure S12 Photothermal effect under 808 nm laser irradiation for 400 s (a) with Au@CZIF of different concentrations and laser power density of 1 W $cm^{-2}$ or (b) with 2 mg $mL^{-1}$ Au@CZIF and different laser power densities. (c) Heating and cooling curves of Au@CZIF aqueous solution (100 μg $mL^{-1}$) under laser irradiation (2 W $cm^{-2}$). Linear time data obtained from the cooling period was used to calculate photothermal conversion efficiency. (d) Photothermal stability.

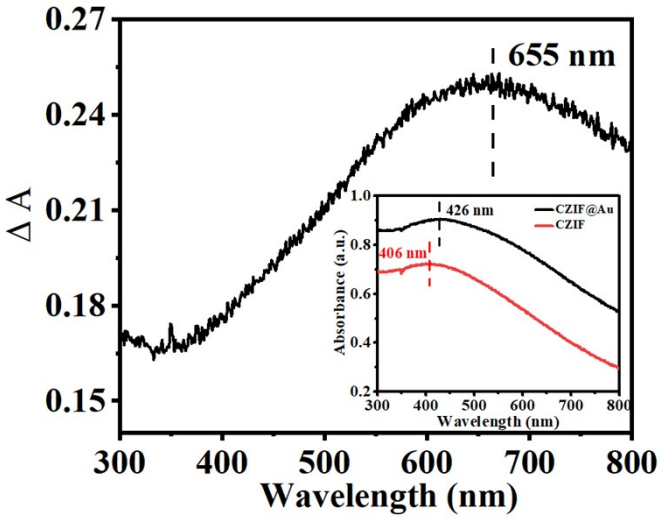


Figure S13 Absorbance of the Au NPs loaded on CZIF. The inset shows solid UV-*vis* absorption spectra of CZIF/Au and CZIF.

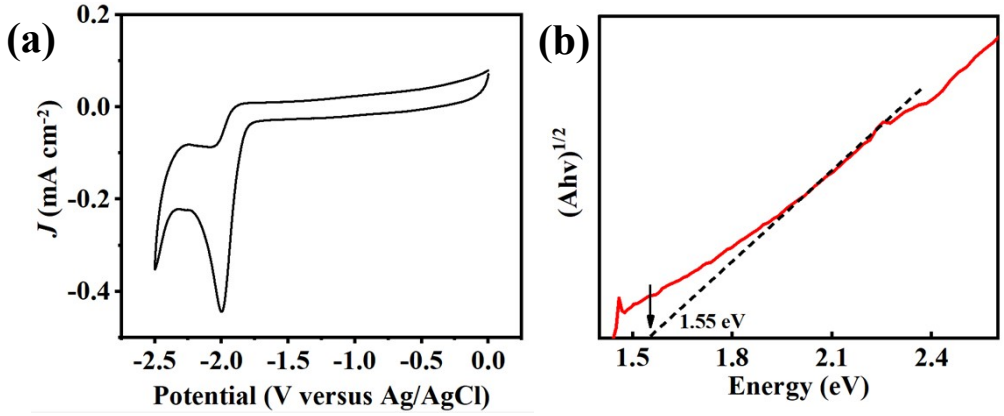


Figure S14 (a) Cyclic voltammogram of CZIF in a solution of 0.1 M $CH_3CN$ under $N_2$ atmosphere at a scan rate of 30 mV/s. The LUMO energy levels is calculated from the onset reduction potential ($E_{red}$) using the following equation: $E_{LUMO} = -(E_{red} + 4.71)$ eV. The onset reduction potential is located at -1.70 eV *vs*. Ag/AgCl reference electrode. Calibrated with 5 mM ferrocene solution is -1.60 eV. The $E_{LUMO}$ is then calculated as -3.11 eV *vs* Vacuum level. (b) The band gap of CZIF is determined to be 1.55 eV by extrapolating the linear region of the absorbance spectrum sub-duplicate.

Table S1 Analysis data of $N_2$ adsorption-desorption isotherms of as-prepared materials. BET surface area ($S_{BET}$) and pore volumes ($V_{pore}$) are calculated based on BET and Barrett-Joyner-Halenda (BJH) methods, respectively.

| Catalyst | $S_{BET}$ ($m^2$ $g^{-1}$) | $V_{pore}$ ($cm^3$ $g^{-1}$) |
|---|---|---|
| ZIF-8 | 1771 | 0.63 |
| ZIF-8@$SiO_2$ | 1418 | 0.62 |
| ZIF-8@$SiO_2$-800 | 44 | 0.08 |
| CZIF-800 | 671 | 0.14 |
| CZIF/Au | 973 | 0.86 |